International Journal of GEOMATE, Aug., 2021, Vol.21, Issue 84, pp.188-193
ISSN: 2186-2982 (P), 2186-2990 (O), Japan, DOI: https://doi.org/10.21660/2021.84.j2179
Geotechnique, Construction Materials and Environment

IDENTIFICATION OF ROCK LAYER CONTACTS IN THE SURROUNDING OF THE SUTAMI DAM USING GEOMAGNETIC METHODS

*Muwardi Sutasoma[1], Adi Susilo[1], Sunaryo[1], Sarjiyana[2], Rifko Harny Dwi Cahyo[3]and Eko Andi Suryo[4]

[1] Faculty of Science, Brawijaya University, Indonesia
[2] Department of Mechanical Engineering, State Polytechnic of Malang, Indonesia
[3] Faculty of Science, Billfath University, Indonesia
[4]Faculty of Engineering, Brawijaya University, Indonesia.

*Corresponding Author, Received: 23 April 2021, Revised: 27 May 2021, Accepted: 13 June 2021

ABSTRACT: Research on rock layer contact at Sutami Dam, Karangkates Village, Sumberpucung District, Malang Regency, Indonesia was undertaken. This research was conducted to identify volcanic sediments layers' which contact with Limestone Sediments in the surrounding of Sutami Dam and to mitigate potential disasters in the dam's surrounding area. This research was conducted by a geomagnetic method. Data were collected using the Proton Precession Magnetometer G-856. The geomagnetic data acquisition started from the Kromengan District (112.494ºE; 8.129ºS) to the Sukorame District (112.358ºE; 8.213ºS). The radius of geomagnetic data acquisition was 15 km; the space between the points was 300 meters with 1372 measurement points. The value of the geomagnetic intensity are between -210 nT to 514 nT. The northern part of the research location has a lower total geomagnetic intensity than the southern area. The northern part is thought to be volcanic sediment (Tuff Desposits and Butak Volcanic Sediments), which only covers the surface, while the southern part is (Limestone Sediments) Marine sediment, which is some parts thought to have been volcanoes in ancient times. The ancient volcanoes in the southern part are Mounts Golo, Selorejo, Selumban, Tretes, Soko, Pehlembun and Krowedul. The contact layer between volcanic sediments with Limestone Sediments is more difficult to consolidate, so that the buildings built on them are more vulnerable.

Keywords: A rock Layer Contacts, Sutami, Geomagnetic, Total Geomagnetic Intensity

1. INTRODUCTION

Sutami Dam is a dam located in Karangkates Village, Sumberpucung District, Malang Regency, East Java Province, Indonesia. It is located at 188-387 m asl (above sea level), has a embankment length of 800 m and a width of 13.7 m. This dam was built in 1964 to 1973, and began operating in 1977 [1].

Sutami Dam is an essential infrastructure in East Java Province. It is used to accommodate excess rainwater and water discharge from the Brantas River to meet water needs in the dry season [2]. In addition, Sutami Dam is also used as a Hydroelectric Power Plant, tourist attractions, and flood control. The north of the Sutami Dam, there is a Lahor Dam, which was built in 1972, and started operating since November 1977. Both the Sutami and the Lahor Dams, located in Karangkates Village, have generated around 400 kWh of electricity per year [3]. The total demand of electricity in Indonesia is around 52,263.06 MW [4]. As a vital hydropower plant in Indonesia, to maintain dam safety and energy sustainability, the dam's subsurface structure must be considered. This is because dam safety is influenced by subsurface geological aspects [5] and hydrostatic pressure.

Hydrostatic pressure affects the contact of the subsurface soil layer and its magnitude depends on the depth of a compressive area at a certain depth [6]. Dams have high hydrostatic pressure due to the presence of surface water, so it is necessary to investigate the type of subsurface soil layer.

Dams located in homogeneous areas are more resistant to hydrostatic pressure than the dams located in non homogeneous areas. In homogeneous areas, the gaps between the layers that are filled with water will reduce cohesion and increase lateral pressure due to hydrostatic pressure [6]. Based on the geological map, the Sutami Dam is located in heterogeneous area, namely the contact area between limestone and andesite lava deposits [7]. So further research is needed. Moreover, The Sutami Dam is Located in the shear fault area around Pohgajih [6] and is also in an earthquake-prone area [1]. As a result, subsurface structures and geological conditions are crucial to determining the Dam's vulnerability.

Determining the subsurface structure and its geological conditions are necessary to be investigated using geophysical method [8]. The method used to determine the subsurface structure around the Sutami Dam is geomagnetic (geomagnetic). This method is used to measure of

rocks' magnetic properties below the surface, which is influenced by its geomagnetic field.

The geomagnetic method is based on the measurement of geomagnetic anomalies caused by differences in geomagnetic susceptibility contrast. Different rock types will provide different rock susceptibility properties [8]. The geomagnetic method can also explain the kind of general subsurface rock layer [9]. Beside that, geomagnetic methods can determine subsurface depth and structure, that can obtain a clearer local and regional anomalies [10].

Therefore, it is necessary to conduct research using geomagnetic methods to detect the sedimentary rock layers' contact in the Sutami Dam area. The results of this study can be used as recommendations for the government to determine policies in disaster mitigation.

2. FIELD SITE STUDY

Sutami Dam is located in the geological map of Wlingi (Figure 1) [11]. The types of rock in this area are lapilli tuff, pumice, and lava tuff.

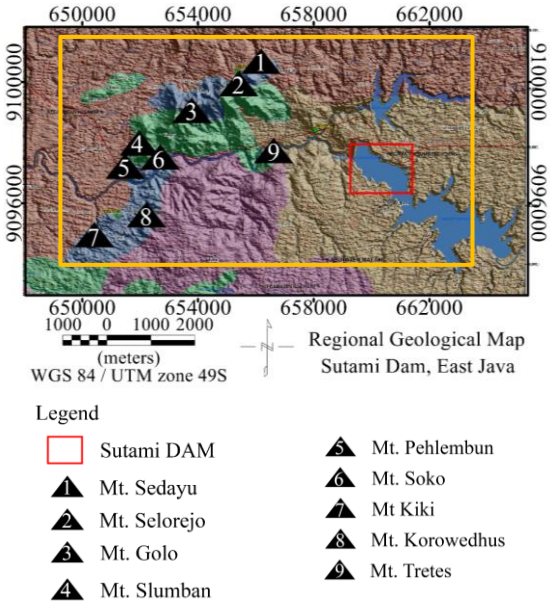

Fig. 1 Research Area (Mark in Yellow) on Geological Map of Wlingi.

Regionally, there are six rock formations, namely Butak volcanic deposits (Qpkb), Campurdarat Formation (Tmcl), Nampol Formation (Tmn), Wuni Formation (Tmw), Mandalika Formations and tuff deposits (Qptm). These formations, two of which are included in the surface sediment category, namely the Campurdarat Formation and the Nampol Formation. Meanwhile, four other formations are included in the category of volcanic rock, namely the Wuni Formation, the Butak Volcano Sediment, the Tuff Deposit and the Mandalika Formation [6]. The dam site was also surrounded by the Pohgajih Local Shear Fault, the Selorejo Local fault, and the Selorejo limestone-andesite contact area [12].

3. METHOD

3.1 Geomagnetic Data Acquisition

This research was conducted in October-November 2019, starting from the Kromengan area, (112.494ºE; -8.129ºS) to the Sukorame area (112.358ºE; -8.213ºS). The area of the research location is 15 km x 15 km, with point intervals of 300 m. The number of magnetic stations was 1372 points. Geomagnetic data retrieval was performed using a Proton Procession Magnetometer (PPM) type G-856. Data retrieval includes latitude, longitude, altitude, time, and geomagnetic variations in nano-Tesla (nT).

3.2 Geomagnetic Data Processing

3.2.1 Diurnal Correction

Temporary changes in the earth's geomagnetic field must be considered to obtain an accurate value. Diurnal correction is a correction performed to correct temporary changes in the earth's geomagnetic field. Diurnal correction occurs due to deviations in the value of the earth's geomagnetic field, caused by solar radiation's effects during the day. Earth's geomagnetic field values can be different between the day and night, eventhough in the same position. The daily variation recorded at a particular time of the geomagnetic field data and can be written as,

$$H_{Day} = \frac{t_n - t_{bs}}{t_{ak} - t_{bs}} (H_{ak} - H_{bs}) \quad (1)$$

where H_{Day} is the intensity of the diurnal geomagnetic field, H_{ak} is the intensity of the geomagnetic field on the last point, H_{bs} is the intensity of the geomagnetic field at the base station, t_n indicates the time measurement at the suitable measuring point, t_{bs} is the time measurement in the base station and t_{ak} is the measurement time point of the last day.

3.2.2 IGRF Correction

IGRF (International Geomagnetic Reference Field) Correction is a general model of spherical harmonics of the earth's geomagnetic field that is sourced from an internationally agreed upon the core [13]. This study uses the value IGRF on the year 2019. After the IGRF correction is obtained, the total geomagnetic field anomalies can be calculated by reducing the value of the measured geomagnetic intensity field by the diurnal

correction and IGRF correction which can be written as,

$$\Delta H = H_{obs} - \Delta H_{Day} - H_o \quad (2)$$

where ΔH is the intesity of total geomagnetic field anomaly, H_{obs} is the measured intensity of the magnetic field, and H_o is the geomagnetic field induced by IGRF.

3.2.3 Upward Continuation transformation and Pseudogravity Transformation

a. Upward Continuation Transformation

Upward continuation transforms a potential field measured on a surface to another surface area far from the source. The aim is to reveal anomalies caused by deeper sources or eliminate anomalies caused by shallow sources [14]. The Fourier transform for this method can be written as,

$$F[U_u] = F[U]F[\varphi_u] \quad (3)$$

$$\varphi_u(x, y, \Delta z) = \frac{\Delta z}{2\pi} \frac{1}{(x^2 + y^2 + \Delta z^2)^{3/2}} \quad (4)$$

$F[U_u]$ is an upward continuation transformation, $F[U]$ is the transformation of the geomagnetic anomaly data, and $F[\varphi_u]$ is the transformation of the constant φ_u depending on x, y and Δz.

b. Pseudogravity Transformation

Pseudogravity is used to change the previously dipole's geomagnetic anomaly to monopole as if it were a gravity anomaly [15]. The pseudogravity transformation can strengthen the subsurface structure analysis by calculating the magnetization value ratio to the pseudo-density value. Poisson' relation is the basic principle of this transformation, where Poisson' relation can be written as,

$$V = -\frac{C_m}{\gamma\rho} M\hat{m} \cdot \nabla_p U \quad (5)$$

$$= \frac{-C_m M g_m}{\gamma\rho} \quad (6)$$

where V is the geomagnetic potential, U is the potential gravity (m^2/s^2), g_m is the component of gravity in the direction of magnetization, γ is the Newton constant, ρ is the rock density (kg/m^3), C_m is the geomagnetic constant, M is the magnetization (Ampere/meter).

3.2.4 Reduction to The Pole (RTP)

The process of reduction to the poles was made because the magnetic anomaly has negative and positive polarity unlike the monopole gravity anomalies. The reduction to the poles is used to eliminate the magnetic anomaly data from the distorting effects of the variating azimuthal tendency of the magnetization vector [13]. In the research area, the declination is -5.45^0 and the inclination is -29.83^0.

3.3 Data Interpretation

The interpretation of geomagnetic data is through a qualitative and quantitative approach. Qualitative interpretation is based on the contour pattern of geomagnetic field anomalies that originate from the distribution of magnetized objects below the earth's surface. In contrast, quantitative interpretation is carried out by making models of residual anomalies.

4. RESULT AND DISCUSSION

The data interpretation used qualitative and quantitative methods. Qualitative methods are used to determine the type of anomaly by reading the contours of the geomagnetic anomaly. Quantitative methods are used to determine the type of subsurface layer obtained by modeling and adjusted to the study area's geological map.

4.1 Total Geomagnetic Intensity Map

The total geomagnetic intensity map illustrates the average value of geomagnetic susceptibility in the study area and shows the bedrock's lithology and topography. Reducing the study area's dipolar nature also requires the total geomagnetic Intensity to be reducted to the poles. The total geomagnetic intensity map (Figure 2) has a minimum value of -210 nT and a maximum value of 554 nT.

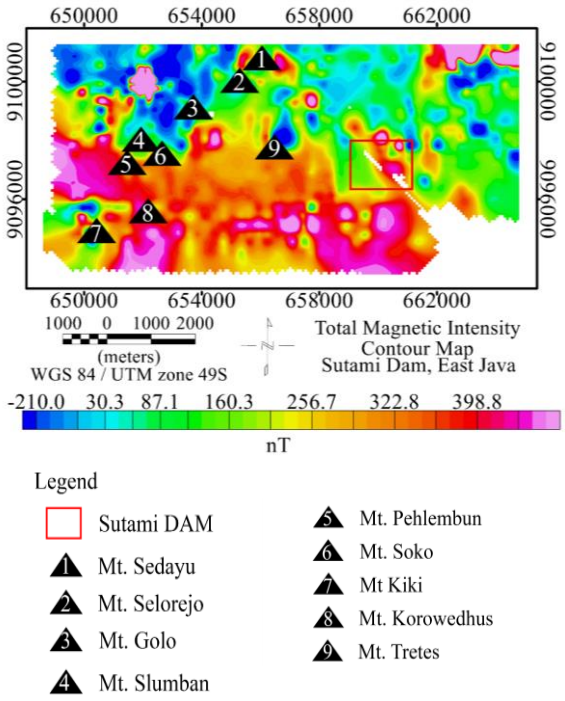

Fig. 2 Total Geomagnetic Intensity Map

Based on the range of anomaly values on the total geomagnetic intensity map, anomalies can be grouped into two groups, namely low anomalies, and high anomalies. The high anomaly in the southern part is indicated by the value range of 226.7 nT to 554.0 nT. This anomaly is estimated as andesite to basalt and latite porphyry from the Mandalika Formation (Tomm), with tuff members of the Mandalika Formation (Tomt) which are composed of dacite and rhyolite. The two have an interfingering correlation. The ages of these two units are estimated to be Late Oligocene or possibly to the Early Miocene. The Mandalika Formation stretches approximately 15 km from the south coast of Blitar. Moreover, a high anomaly in the Northeast is thought to be part of the Mount Kawi lava dome.

Low anomaly is in the northern part with a value range of -210 nT to 209.5 nT. This anomaly is a combination of several formations, consisting of the Campurdarat Formation, the Wuni Formation and the Nampol Formation. The Campudarat (Tmcl) formation consists of limestone and clay rock. The Wuni Formation (Tmw) consists of breccias, lava, andesite-basalt lava with coarse to fine tuffaceous sandstones. The Nampol Formation (Tmn) consists sandstone, sandstone clay, sandstone, tufan sandstone, and limestone sandstone.

4.2 Regional Geomagnetic Map

Regional geomagnetic map (Figure 3) are obtained after low pass filtering of total geomagnetic Intensity. High-frequency anomalies and noise in total geomagnetic Intensity to be filtered out. Only low-frequency anomalies remain to indicate a deep source [16]. The regional geomagnetic map is stable and reflect the study area's regional structure when there are no positive and negative closure pairs. Figure 4 shows a map of regional anomalies with values ranging from -14.5 nT to 461.1 nT. The geomagnetic anomaly value in the south of the study area was higher than the north.

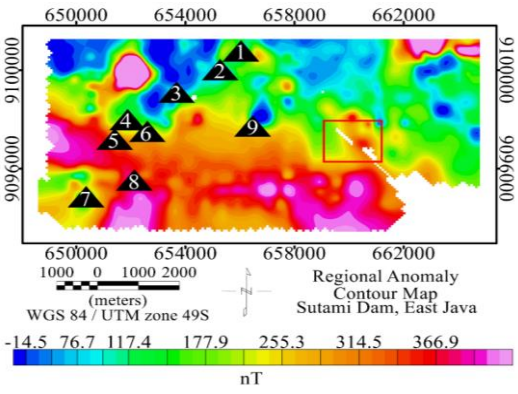

Fig. 3 Regional Geomagnetic Map

4.3 Residual Geomagnetic Map

The residual anomaly is obtained after performing a high pass filter on the total geomagnetic intensity. The residual geomagnetic map (Figure 4) has a values ranging from -296.9 nT to 141.0 nT. This value indicates that the variation of rock susceptibility is related to the geology of the study area.

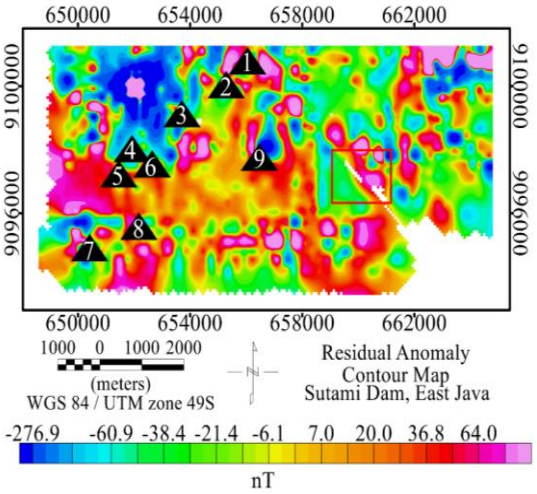

Fig. 4 Residual Geomagnetic Map

The residual anomaly map (Figure 4) shows that the south's geomagnetic field value is higher than the north. The contact of the rocks between the Kawi Butak volcanic sediments and marine sediments (limestone sediments) can be seen clearly. The northern side in Figure 5 is estimated to be Kawi sediment and only covers the top of the rock. In contrast, the south side is marine sediment with a higher geomagnetic field value because this side is thought to have been volcanoes in ancient times. Ancient volcanoes in the southern part include Mount Selumban, Mount Soko, Mount Tretes, Mount Kiki, Mount Pahlembun and Mount Korowedhus.

4.4 Pseudogravity Transformation

Pseudogravity is used to change the previous dipole's geomagnetic anomaly to monopole gravity anomaly. The pseudogravity transformation results will strengthen the subsurface structure analysis by calculating the magnetization value's comparability to the apparent density value. The results of pseudogravity can be seen in Figure 5.

The pseudogravity map (Figure 5) has a minimum value of -0.2 mGal and a maximum of 0.5 mGal. The high anomaly in the northwest and north of the study area is volcanic deposits (Tuff) originating from Mount Selorejo, Mount Sedayu, and Mount Golo. In comparison, the Southern Part is volcanic deposits from Mount Tretes. In the

Northeast, areas with high anomalies are still related to the sediments of Mount Kawi.

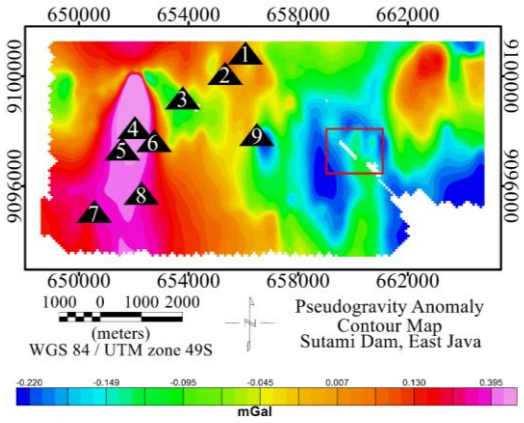

Fig. 5 Pseudogravity Map

4.5 2D Profile in the Study Area

Quantitative interpretation of the study area can be made by making a slice on the residual anomaly. There are three line of slicing: Slice a-a', a Slice b-b', and Slice a c-c '. The location of the slice can be seen in Figure 6.

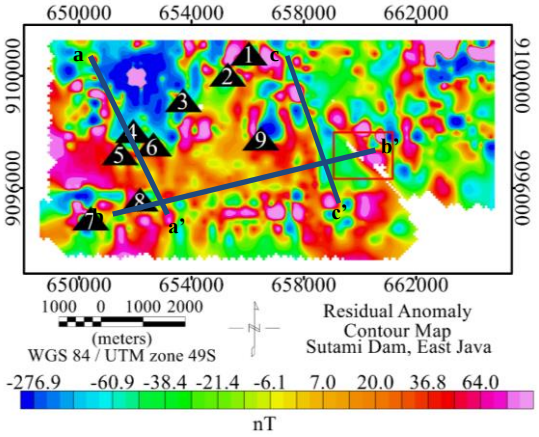

Fig. 6 Slice on Residual Geomagnetic Map

The results of subsurface modeling on the slice a-a' can be seen in Figure 7. There are six formations in the Slice a-a', namely Volcanic Products, Wuni Formation, Mandalika Formation, Campurdarat Formation, Nampol Formation dan Soil. This area has ancient volcanoes, namely Mount Soko and Pahlembun, causing the Wuni Formation to be cut off by Campurdarat Formation and reappearing on the surface at a distance of 2400-300 meters and a depth of 0-100 meters. The contact layer of the limestone and volcanic sediments is located between the Tuff Deposits with the Wuni Formation and the Campurdarat Formation. Generally, the Wuni and Campurdarat Formations are below the Tuff Deposit so that they get a bigger load and are more consolidated than above one [7].

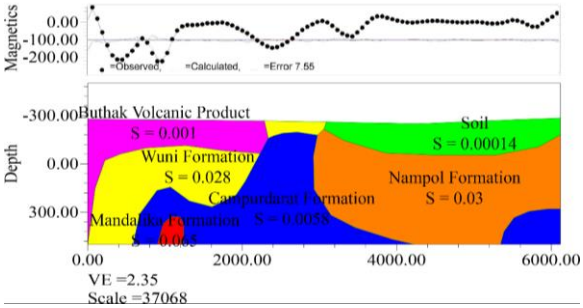

Fig 7. 2D Profile a-a'

The results of subsurface modeling in the Slice b-b' can be seen in Figure 8. There are four formations in the Slice b-b', namely soil, Campurdarat Formation, Nampol Formation and Tuff Deposits. The contact layer between limestone and volcanic sediments is located between the Nampol Formations and the Tuff Deposits. Generally, The Nampol Formation is below the Tuff Deposit so this formation gets a bigger load and is more consolidated than above [7]. Therefore, the two layers of contact becomes more vulnerable. This results in a weak zone in the area, bodies and embankments of the Sutami Dam [17]. As well as the emergence of a fracture zone in the dam area that spreads upstream, downstream of the main road is also at the top of the dam [3].

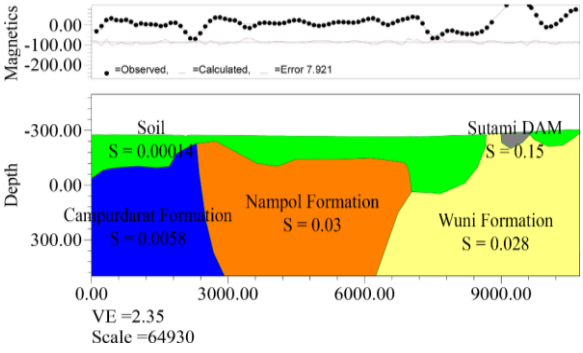

Fig 8. 2D Profile b-b'

The results of subsurface modeling on the slice c-c' can be seen in Figure 9. There are four formations in the slice c-c' namely soil, Butak the Volcanic Products, the Tuff Deposits and the Campurdarat Formations. The contact layer of limestone with volcanic sediments is located at the Tuff Deposits and the Campurdarat Formation. Generally, The Campurdarat Formation is below the Tuff Deposit so this formation gets a bigger load and is more consolidated than above one [7]. The contact layer between these two types of formations is more difficult to consolidate. So that, the buildings built on it become more vulnerable.

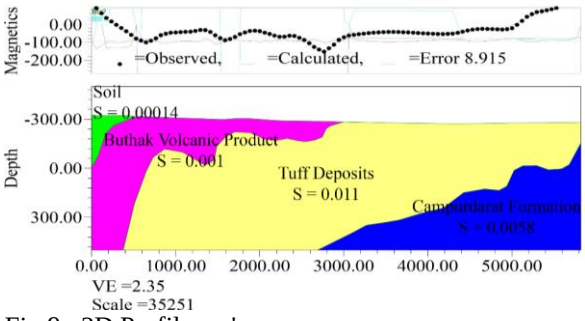

Fig 9. 2D Profile c-c'

5. CONCLUSION

The value of the geomagnetic field in the south is higher than in the north. The north side is thought to be Butak Kawi sediment, where the sediment only covers the surface. On the other hand, the south is marine sediment with a higher geomagnetic field value as it was suspected to be an ancient volcano. These ancient volcanoes are Mount Golo, Mount Selorejo, Mount Selumban, Mount Tretes, Mount Kiki, Mount Soko, Mount Pehlembun and Mount Krowedul.

This research indicates that the rock contact layer between volcanic sediments layers' contact with Limestone Sediments is at the boundary between tuff deposit and Campurdarat formations. Tuff deposits formed in the late Plistocene to early Holocene during the Quaternary period have rock types that have not fully consolidated. Meanwhile, the mixed tertiary layers formed in the early Miocene of the Tertiary era have perfectly condensed rock types. The contact layer between these two types of formations is more difficult to consolidate, so that the buildings built on them are more vulnerable.

As explained above, that the dam is built in the non homogeneous sediment. The government should pay more attention and evaluation, regarding this condition.

6. REFERENCES

[1] Purwana Y. M., Raden Harya D.H.I, Setiawan B., and Aulawi N., Seismic Hazard Analysis for Sutami Dam using Probabilistic Method. *MATEC Web of Conferences*, vol. 12, 2019, pp. 1–9.

[2] Irvani H., Bisri M., and Soetopo W., Studi optimasi pola operasi waduk sutami akibat perubahan iklim, *J. Tek. Pengairan*, vol. 4, issue 2, 2012, pp. 1-9

[3] Sunaryo and Susilo A., Seepage Zone Identification at Sutami Dam by Means of Geoelectrical Resistivity Data, *IOP science*, Vol. 012011, Issue 75, 2017, pp. 1–6.

[4]https://web.pln.co.id/statics/uploads/2021/04/Statistik-Indonesia-2020-unaudited.pdf 2021 acces date 18 March 2021

[5] Jannah L., Basid A., and Rusli, Pendugaan Bidang Gelincir Tanah Longsor Berdasarkan Sifat Kelistrikan Bumi dengan Aplikasi Geolistrik Metode Tahanan Jenis, *J. Neutrino*, Vol. 3, Issue 1, 2010, pp. 66–76.

[6] Hardiyatmo, Hary C., Mekanika Tanah 2, Gadjah Mada University Press, 2012, pp.200-282.

[7] Sjarifudin S. and Hamidi, Peta Geologi Lembar Blitar, Jawa. Pusat Penelitian dan Pengembangan Geologi, Bandung, 1992.

[8] Telford W. M., Geldart R. E., and Sheriff L.P., Geomagnetic Methods, in *Applied Geophysics*, Cambridge University Press, 1990, pp. 62-135.

[9] Reynolds J. M., An introduction to Applied and Environmental Geophysics, John Wiley and sons, 1997, pp. 83–136.

[10]Burger H. R., Sheehan A. F., and Jones C., Introduction to Applied Geophysics: Exploring the Shallow Subsurface, prentice Hall PTR, 1992, pp. 389–452.

[11] Suwijanto, Peta Geologi Hasil Inderaan Jauh Wlingi, Jawa Timur. Badan Geologi Pusat Survei Geologi Kementrian Energi dan Sumber Daya Mineral, Bandung, 2013.

[12]Sunaryo and Susilo A., Vulnerability of Karangkates Dams Area by Means of Zero Crossing Analysis of Data Geomagnetic, in *AIP Conference Proceedings*, Vol. 060007, 2015, pp. 1–8.

[13]Susilo A., and Sunaryo, Investigation of Sidoarjo Mud Volcano (‘LUSI’) Impact on the Subsurface using Geomagnetic Method at Sidoarjo District, Indonesia, *Disaster Adv.*, Vol. 11, no. 3, 2018. pp. 1–8,

[14] Blakely R. J., Potential Theory in Gravity and Geomagnetic, Cambridge University Press, 1995, pp. 313–356.

[15] Subarsyah S. and Priohandono Y. A., Metoda Pseudo-Gravity Dalam Analisis Kelurusan Dan Patahan Di Sekitar Tinggian Asahan, Perairan Selat Malaka, *J. Geol. Kelaut.*, Vol. 7, Issue 2, 2016, pp. 65–71.

[16] Chian O. W., Zakariah M. N. A. B., Rafek A.G. B.M., Mohamed M. A, Delineation of Subsurface Structures of Semanggol Formation, North Perak using Geomagnetic Data, International Journal of GEOMATE, Vol. 17, Issue 59, 2019, pp. 204–209.

[17] Sunaryo and Susilo A.,Vulnerability of Karangkates Dams Area by Means of Density Contrast Parameter to Anticipate Energy Sustainability, in *Basic Science*, Vol. 5. Issue 9, 2015, pp. 1689–1699.